
An unconditionally stable method for air motion inside cylinders

864

Gerardo Abrugia

Received August 1997
Revised November 1997
Accepted June 1998

Dip. Matematica e Applicazioni, "R. Caccioppoli", Università di Napoli, "Federico II", Italy and CNR, Istituto Motori, Napoli, Italy, and

Umberto Amato

Istituto per Applicazioni della Matematica, CNR, Napoli, Italy

1. Introduction

In the last few years in the scientific literature there has been a growing interest toward numerical simulation of in cylinder phenomena in internal combustion engines due to the improvements both in computer technology and in the numerical methods. This has been made possible also by the availability of more sophisticated experimental activities, that improved consistently the understanding of the main basic phenomena and allowed more reliable numerical results.

Some multidimensional codes, like KIVA (Amsden *et al.*, 1989), FIRE (Johns, 1984), EPISO (Issa, 1986), adopted by the motor industries, were developed by different schools and are continuously upgraded by the scientific community. In spite of these significant efforts, multidimensional methods still need further progress, both in terms of basic physical knowledge and of computational efficiency: the goal is to obtain a numerical engine useful to designers to develop fully or improve the engine combustion system without time consuming field experiments.

One of the main problems to solve is the availability of numerical methods able to reduce computing time, which is very high for these kind of applications: the goal is the capability to simulate also on low cost machines problems in computational domains with about 10^6 grid points.

The present paper is focused on this topic and discusses a new numerical method that seems able to treat very large grids. An important goal for such numerical methods seems to be the achievement of unconditionally stable fast methods that allow one to choose the time step not constrained by CFL conditions for the fluid velocity and sound speed. Presently many researches are devoted to this objective (see, e.g. EPISO (Issa, 1986)).

In the present paper we propose a numerical method having the following objectives:

- (1) unconditional stability, reached by means of semi-lagrangian techniques (Casulli, 1987); these are not new in the framework of PDE, but do not seem to be widely used in the engine problem;

- (2) satisfaction of as many physical properties of the quantities as possible (positivity, conservation and monotonicity); this task will be accomplished by relying mainly on non linear approximations based on FCT (Boris and Oran, 1987); indeed FCT algorithms are not recent; however in the last years there is a renewed interest toward them due to the high degree of parallelism reachable;
- (3) computational efficiency; to this purpose the numerical method will involve systems of equations whose matrices have nice properties from the mathematical point of view. This guarantees stability of the numerical solution and a very fast solution of the system of equations.

The present paper (and corresponding code) is not intended to compare with the more famous and general codes used by the automotive industry community from an operative point of view, but it wants to give a contribution to the feasibility of unconditionally stable methods in solving the engine problem.

We shall be concerned with Euler's equations (i.e. we shall neglect diffusion). In other words we are assuming that air viscosity can be neglected in the inner part of the domain. This does not affect the feasibility of the numerical method, since convective terms are the most difficult with which to deal. Moreover we consider a 2D Cartesian geometry; extension to the 3D case or cylindrical coordinates is immediate.

2. The equations

Evolution of the system inside a cylinder is governed by Navier-Stokes equations. In the present paper we assume that Euler equations are adequate to describe the system. This is a good approximation due to the small value of air viscosity with respect to the typical velocities involved. Moreover, the convective-advective terms of the Navier-Stokes equations are the most difficult to deal with numerically, so that inclusion of viscosity terms, if needed for more complicated systems, is not a major problem. Therefore, the equations we shall assume for our system are (in the 2D case, for simplicity):

$$\left\{ \begin{array}{l} \frac{\partial \rho}{\partial t} + \frac{\partial(\rho u)}{\partial x} + \frac{\partial(\rho w)}{\partial z} = 0 \\ \frac{\partial(\rho u)}{\partial t} + \frac{\partial(\rho uu)}{\partial x} + \frac{\partial(\rho uw)}{\partial z} = -\frac{\partial P}{\partial x} \\ \frac{\partial(\rho w)}{\partial t} + \frac{\partial(\rho wu)}{\partial x} + \frac{\partial(\rho ww)}{\partial z} = -\frac{\partial P}{\partial z} \\ \frac{\partial E}{\partial t} + \frac{\partial[(E+P)u]}{\partial x} + \frac{\partial[(E+P)w]}{\partial z} = 0 \end{array} \right. \quad (1)$$

endowed with the state equation

$$P = (\gamma - 1) \rho \varepsilon$$

and suitable initial and boundary conditions compatible with Euler equations. Everywhere ρ is density, $\mathbf{q} \equiv (u, v)$ velocity, P pressure, $E = \rho \varepsilon + \frac{1}{2} \rho |\mathbf{q}|^2$ total energy density, γ specific heat ratio and ε specific internal energy. Equation (1) is expressed in conservative form. In the 3D case equations are extended accordingly.

The lower boundary of the cylinder is moving with the piston, so that the boundary conditions have to suitably take account of this and numerical methods have to include a mechanism of moving and shrinking or dilating cells, generally worked out by means of a suitable rezoning procedure. While this could be desirable for some purposes (e.g. adaptivity of the space discretization), however rezoning has some drawbacks (arbitrariness of the averaging or interpolating procedure, need of storing information concerning position of cells dependent on time) which breaks down efficiency of a code.

In the present paper we make a previous transform from the original (physical) moving domain to a (computational) fixed one. This allows one to deal with a grid independent of time, which makes codes more efficient. Indeed mapping (non conformal, in general) into a simpler computational domain is used in many numerical methods for the engine problem but only when faced with non structured grids. To transform the domain also in the case of Cartesian grids has the advantage to solve a problem with the same mathematical and numerical complexity, but with bigger computational efficiency; moreover, interpolation of quantities across the grid is more accurate and, when desired, space adaptivity of the grid can be implemented more easily.

In order to preserve the general form of equation (1) and keep on expressing them in a conservative way, a conformal mapping has been resorted (Thompson *et al.*, 1985). More precisely, if (x, z) , (ξ, ζ) are co-ordinates in the physical and computational domains, respectively, then the transform we consider is

$$\begin{cases} \xi = x \\ \zeta = z - z_t, \quad \text{for } z_t \leq z \leq z_t + z_{bowl} \end{cases} \quad (2)$$

and

$$\begin{cases} \xi = x \\ \zeta = z_{bowl} \frac{z - z_t - z_{bowl}}{z_{top} - z_t - z_{bowl}} (z_{top} - z_{bowl}), \quad \text{for } z_t + z_{bowl} < z \leq z_{top}, \end{cases} \quad (3)$$

where (see Figure 1).

- (1) z_t is position of the piston (also bottom of the bowl), time depending;
- (2) z_{bowl} is height of the bowl;
- (3) z_{top} is position of the top of the cylinder (also height).

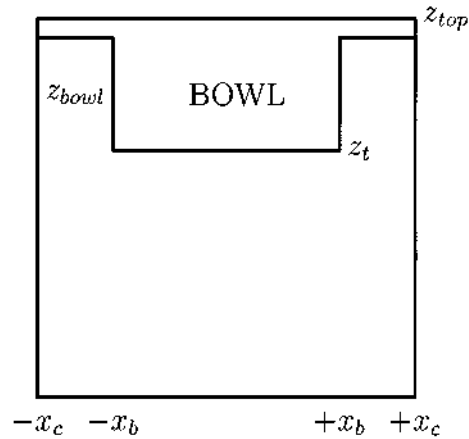


Figure 1.
Physical moving
domain

Transform (2) and (3) is clearly conformal. Therefore, making use of the rules for transforming equations by a conformal mapping (Thompson *et al.*, 1985), while preserving the conservative form, equation (1) results in

$$\left\{ \begin{array}{l} \frac{\partial R}{\partial t} + \frac{\partial(Ru)}{\partial x} + \frac{\partial(RW)}{\partial \zeta} = 0 \\ \frac{\partial(Ru)}{\partial t} + \frac{\partial(Ruu)}{\partial x} + \frac{\partial(RuW)}{\partial \zeta} = -\sqrt{g} \frac{\partial P}{\partial x} \\ \frac{\partial(Rw)}{\partial t} + \frac{\partial(Rwu)}{\partial x} + \frac{\partial(RwW)}{\partial \zeta} = -\frac{\partial P}{\partial \zeta} \\ \frac{\partial(\sqrt{g}E)}{\partial t} + \frac{\partial[\sqrt{g}(E+P)u]}{\partial x} + \frac{\partial[\sqrt{g}(E+P)W]}{\partial \zeta} = -\frac{\partial(Pw_{grid})}{\partial \zeta} \end{array} \right. (4)$$

where $R = \sqrt{g} \rho$ is computational density, w_{grid} grid velocity, \sqrt{g} is defined as

$$\sqrt{g} = \begin{cases} 1, & \text{for } z_t \leq z \leq z_t + z_{bowl} \\ \frac{z_{top} - z_t - z_{bowl}}{z_{top} - z_{bowl}}, & \text{for } z_t + z_{bowl} < z \leq z_{top} \end{cases}$$

and $\mathbf{Q} \equiv (U, W)$ is computational velocity, whose components are defined as

$$\begin{aligned} U &= u \\ W &= \frac{1}{\sqrt{g}} (w - w_{grid}) \end{aligned} \quad (5)$$

In the case of 3D domain, the conformal mapping (2) and (3) is completed by the transform $\eta = y$, $z_t \leq z \leq z_{top}$ with y, η being co-ordinates in the physical and computational domains, respectively.

3. The numerical method

In the present section we derive a numerical method for approximating equation (4) in the computational domain. We shall assume that the physical (moving) domain

$$D = [-x_b, x_b] \times [z_t, z_t + z_{bowl}] \cup [-x_c, x_c] \times [z_t + z_{bowl}, z_{top}]$$

mapped into the computational (fixed) domain

$$T = [-x_b, x_b] \times [0, \zeta_{bowl}] \cup [-x_c, x_c] \times [\zeta_{bowl}, \zeta_{top}]$$

by transform (2) and (3) (see Figures 1 and 2 for the legenda of symbols).

The staggered grid, shown in Figure 3, is considered for the approximation of the equation (4); in particular the thermodynamic variables (density, pressure, energy) are defined at the center of the computational cells, (x_i, ζ_k) , whereas horizontal and vertical velocities are defined at the right and left (upper and bottom, respectively) boundaries, $(x_{i+1/2}, \zeta_k)$ and $(x_i, \zeta_{k+1/2})$, respectively. Moreover, we define the cell boundaries (lengths in the 2D case) $\Delta x_i = x_{i+1/2} - x_{i-1/2}$ and $\Delta \zeta_k = \zeta_{k+1/2} - \zeta_{k-1/2}$; finally the (2D) volume of the cell is defined as $V_{i,k} = \Delta x_i \Delta \zeta_k$. In the 3D case velocity over the y co-ordinate, v , is defined analogously in the staggered grid and $V_{i,j,k}$ is a true 3D volume.

Figure 2.
Computational fixed domain

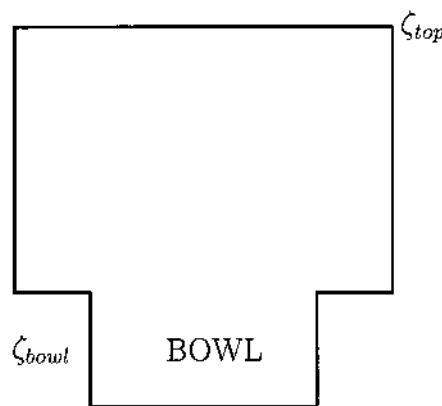
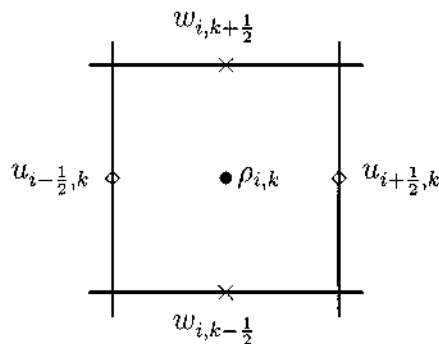


Figure 3.
Staggered grid



Aim of the paper is to provide a numerical method for approximating Euler equation (4) tailored for the engine problem and with the following appealing features:

- Preservation of physical properties of the fluid, namely conservation, positivity, monotonicity. It is well known that this point is addressed in all operative codes for the engine problem for several reasons: from a theoretical point of view the real fluid obeys to laws that preserve those properties; to satisfy them also from the numerical point of view produces meaningful simulations (e.g. density is always positive with monotone numerical methods, discontinuities can be well represented if numerical methods are conservative). When a numerical method satisfies only a few (less restrictive) mathematical requirements (e.g. stability, accuracy), thermodynamic variables can become negative or discontinuities are improperly treated; in this case physical properties are satisfied by resorting computational tricks that de facto degrade accuracy or mathematical properties (in this respect we mention the “robin hood” algorithm for preserving positivity of density, well known to the users of KIVA code). In the present paper physical properties will be mainly preserved by means of a mixed finite difference-finite volume method and by using FCT method.
- Unconditional stability. A major trend of present research for automotive industries is to devise numerical methods unconditionally stable. This allows people to use large time steps and so, hopefully, to reduce the total computational time. We stress that since accuracy of the solution depends directly on the time step (to some power, depending on the order of the method), of course increasing the time step increases truncation error; then large time steps make sense when the general behaviour of air motion is sought, which is the case in many applications to the engine problem. In the present paper stability condition for the flow speed will be removed by treating implicitly the computational density in the mass conservation equation and using a semi-Lagrangian approach for the momentum equations, while, according to (Casulli, 1990; Casulli and Greenspan, 1984; Patnaik *et al.*, 1987), stability condition for the sound speed will be removed by considering pressure implicit in the momentum equations and velocity implicit in the energy equation.

The method is explained in detail in the following sections.

3.1 Mass conservation equation

Let us rewrite mass conservation equation in the integral form

$$\iint_V \frac{1}{\sqrt{g}} \left(\frac{\partial R}{\partial t} \right) dV + \iint_V \frac{1}{\sqrt{g}} (\nabla \cdot R\mathbf{Q}) dV = 0$$

with V referring to a generic cell of the domain. Since \sqrt{g} is constant over the volume cell, we obtain

$$\iint_V \left(\frac{\partial R}{\partial t} \right) dV + \int_{l^+} (R\mathbf{q}) \cdot \mathbf{n} dl + \int_{l^-} (R\mathbf{q}) \cdot \mathbf{n} dl + \int_{l^{\uparrow}} (R\mathbf{q}) \cdot \mathbf{n} dl + \int_{l^{\downarrow}} (R\mathbf{q}) \cdot \mathbf{n} dl = 0 \quad (6)$$

l^+ , l^- , l^{\uparrow} and l^{\downarrow} being right, left, upper and lower boundaries of the cell, respectively. We suppose R constant over the cell and u , W constant along the boundaries; moreover we approximate the temporal derivative by an upwind scheme. Then equation (6) results in

$$\begin{aligned} \frac{\tilde{R}_{i,k} - R_{i,k}^n}{\Delta t} V_{i,k} + \tilde{R}_{i+\frac{1}{2},k} u_{i+\frac{1}{2},k}^n \Delta \zeta_k - \tilde{R}_{i-\frac{1}{2},k} u_{i-\frac{1}{2},k}^n \Delta \zeta_k \\ + \tilde{R}_{i,k+\frac{1}{2}} W_{i,k+\frac{1}{2}}^n \Delta x_i - \tilde{R}_{i,k-\frac{1}{2}} W_{i,k-\frac{1}{2}}^n \Delta x_i = 0 \end{aligned} \quad (7)$$

with

$$\tilde{R}_{i+\frac{1}{2},k} = \frac{1}{2} (\tilde{R}_{i+1,k} + \tilde{R}_{i,k}) \quad \text{and} \quad \tilde{R}_{i,k+\frac{1}{2}} = \frac{1}{2} (\tilde{R}_{i,k+1} + \tilde{R}_{i,k}).$$

The scheme so developed is a classical second order in space finite difference one when applied to a uniform grid and then it is not monotone; in order to keep monotonicity, FCT implicit step is applied. Let

$$\begin{aligned} F_{i+\frac{1}{2},k}^d &= \nu_{i+\frac{1}{2},k} (\tilde{R}_{i+1,k} - \tilde{R}_{i,k}) V_{i+\frac{1}{2},k} \\ F_{i,k+\frac{1}{2}}^d &= \nu_{i,k+\frac{1}{2}} (\tilde{R}_{i,k+1} - \tilde{R}_{i,k}) V_{i,k+\frac{1}{2}} \end{aligned}$$

be implicit diffusive fluxes that are added at the right-hand side of equation (7), with $V_{i+\frac{1}{2},k} = \frac{1}{2} (V_{i+1,k} + V_{i,k})$ and $V_{i,k+\frac{1}{2}} = \frac{1}{2} (V_{i,k+1} + V_{i,k})$ and $\nu_{i,k}$ being diffusive coefficients; then equation (7) can be written as

$$a_{i-1,k} \tilde{R}_{i-1,k} + a_{i,k-1} \tilde{R}_{i,k-1} + a_{i,k} \tilde{R}_{i,k} + a_{i+1,k} \tilde{R}_{i+1,k} + a_{i,k+1} \tilde{R}_{i,k+1} = R_{i,k}^n V_{i,k} \quad (8)$$

where the coefficients $a_{i,k}$ are defined as

$$\begin{aligned} a_{i-1,k} &= -V_{i-\frac{1}{2},k} \left(\nu_{i-\frac{1}{2},k} + \frac{1}{2} \varepsilon_{i-\frac{1}{2},k} \right) \\ a_{i,k-1} &= -V_{i,k-\frac{1}{2}} \left(\nu_{i,k-\frac{1}{2}} + \frac{1}{2} \varepsilon_{i,k-\frac{1}{2}} \right) \\ a_{i+1,k} &= -V_{i+\frac{1}{2},k} \left(\nu_{i+\frac{1}{2},k} - \frac{1}{2} \varepsilon_{i+\frac{1}{2},k} \right) \\ a_{i,k+1} &= -V_{i,k+\frac{1}{2}} \left(\nu_{i,k+\frac{1}{2}} - \frac{1}{2} \varepsilon_{i,k+\frac{1}{2}} \right) \\ a_{i,k} &= V_{i,k} + V_{i-\frac{1}{2},k} \left(\nu_{i-\frac{1}{2},k} - \frac{1}{2} \varepsilon_{i-\frac{1}{2},k} \right) + V_{i,k-\frac{1}{2}} \left(\nu_{i,k-\frac{1}{2}} - \frac{1}{2} \varepsilon_{i,k-\frac{1}{2}} \right) \\ &\quad + V_{i+\frac{1}{2},k} \left(\nu_{i+\frac{1}{2},k} + \frac{1}{2} \varepsilon_{i+\frac{1}{2},k} \right) + V_{i,k+\frac{1}{2}} \left(\nu_{i,k+\frac{1}{2}} + \frac{1}{2} \varepsilon_{i,k+\frac{1}{2}} \right) \end{aligned}$$

and

$$\varepsilon_{i+\frac{1}{2},k} = \left(u_{i+\frac{1}{2},k}^n \Delta t \Delta \zeta_k \right) / V_{i+\frac{1}{2},k}, \quad \varepsilon_{i,k+\frac{1}{2}} = \left(W_{i,k+\frac{1}{2}}^n \Delta t \Delta x_i \right) / V_{i,k+\frac{1}{2}}.$$

Stable method
for air motion
inside cylinders

Positivity condition imposes the constraints

$$\begin{aligned} \nu_{i+\frac{1}{2},k} &\geq \frac{1}{2} \left| \varepsilon_{i+\frac{1}{2},k} \right| \\ \nu_{i,k+\frac{1}{2}} &\geq \frac{1}{2} \left| \varepsilon_{i,k+\frac{1}{2}} \right|. \end{aligned} \quad (9)$$

871

In the bidimensional case, equation (8) is a system of linear equations band-structured with five bands (block tridiagonal, with each block tridiagonal), giving the transported diffused values, \tilde{R} ; it is solved through the CG-stab method. By satisfying constraints (9) with equality sign, an attractive property of the matrix results: each block is decomposable in bidiagonal blocks, so that a suitable direct solver of system (8) could be implemented. Following FCT procedure, raw antidiffusive fluxes are defined

$$\begin{aligned} F_{i+\frac{1}{2},k}^{ad} &= \nu_{i+\frac{1}{2},k} \left(\tilde{R}_{i+1,k} - \tilde{R}_{i,k} \right) V_{i+\frac{1}{2},k} \\ F_{i,k+\frac{1}{2}}^{ad} &= \nu_{i,k+\frac{1}{2}} \left(\tilde{R}_{i,k+1} - \tilde{R}_{i,k} \right) V_{i,k+\frac{1}{2}}, \end{aligned}$$

then corrector fluxes are calculated

$$\begin{aligned} F_{i+\frac{1}{2},k}^c &= S_{i+\frac{1}{2},k} \max \left\{ 0, \min \left[S_{i+\frac{1}{2},k} \left(\tilde{R}_{i+2,k} - \tilde{R}_{i+1,k} \right) V_{i+1,k}, \left| F_{i+\frac{1}{2},k}^{ad} \right|, \right. \right. \\ &\quad \left. \left. S_{i+\frac{1}{2},k} \left(\tilde{R}_{i,k} - \tilde{R}_{i-1,k} \right) V_{i,k} \right] \right\} \\ F_{i,k+\frac{1}{2}}^c &= S_{i,k+\frac{1}{2}} \max \left\{ 0, \min \left[S_{i,k+\frac{1}{2}} \left(\tilde{R}_{i,k+2} - \tilde{R}_{i,k+1} \right) V_{i,k+1}, \left| F_{i,k+\frac{1}{2}}^{ad} \right|, \right. \right. \\ &\quad \left. \left. S_{i,k+\frac{1}{2}} \left(\tilde{R}_{i,k} - \tilde{R}_{i,k-1} \right) V_{i,k} \right] \right\} \\ S_{i+\frac{1}{2},k} &= \text{signum} \left(\tilde{R}_{i+1,k} - \tilde{R}_{i,k} \right) \\ S_{i,k+\frac{1}{2}} &= \text{signum} \left(\tilde{R}_{i,k+1} - \tilde{R}_{i,k} \right). \end{aligned}$$

Final values of density are given by

$$R_{i,k}^{n+1} = \tilde{R} - \frac{1}{V_{i,k}} \left(F_{i+\frac{1}{2},k}^c - F_{i-\frac{1}{2},k}^c + F_{i,k+\frac{1}{2}}^c - F_{i,k-\frac{1}{2}}^c \right).$$

Approximation of density is first order accurate in time and second order in space (provided that grid is uniform and where solution is smooth enough, so that the nonlinear FCT step is not applied). Moreover total mass is conserved throughout the domain.

In the 3D case convective terms are also present in equation (7) for the third co-ordinate analogously to x and ζ ; moreover FCT implicit diffusive and

antidiffusive fluxes are also introduced for the y co-ordinate again analogously to x and ζ ; finally positivity conditions for y is analogous to equation (9) for x and ζ . Note that in the 3D case in equation (7) cell volumes are true tridimensional and cell boundaries are areas, whose values are obtained multiplying the length of the borders of the corresponding co-ordinates. This also applies to the other equations considered in the following sections.

3.2 Momentum equations (predictor step)

Let us consider the scalar momentum equation (x -direction)

$$\frac{\partial(Ru)}{\partial t} + \nabla \cdot (Ru\mathbf{Q}) = -\sqrt{g} \frac{\partial P}{\partial x}$$

that we rewrite in the following (non-conservative) form

$$\frac{d(Ru)}{dt} + Ru \nabla \cdot \mathbf{Q} = -\sqrt{g} \frac{\partial P}{\partial x};$$

it allows one to approximate explicitly the equation in a semi-lagrangian way, overcoming the CFL conditions for the fluid speed. We solve it in two steps in order to improve accuracy. The first one is an explicit (predictor) step: the pressure term is approximated explicitly to obtain the predicted values of u . The following approximation is made

$$\frac{(\widehat{Ru})_{i+\frac{1}{2},k} - (\widehat{Ru})_{i+\frac{1}{2},k}^n}{\Delta t} + (Ru \widehat{\nabla} \cdot \mathbf{Q})_{i+\frac{1}{2},k}^n = -(\widehat{\sqrt{g}})_{i+\frac{1}{2},k} \left(\frac{\partial P}{\partial x} \right)_{i+\frac{1}{2},k}^n, \quad (10)$$

where $\widehat{\cdot}$ indicates the value of variable s calculated at the beginning of the characteristic curve (time t^n) ending at the grid point $(X_{i+1/2}, \zeta_k)$ at t^{n+1} .

Following an analogous procedure, the same approximation is obtained for the momentum equation (z -direction), we omit for brevity. $\tilde{u}_{i+\frac{1}{2},k}$ and $\tilde{w}_{i,k+\frac{1}{2}}$ can be formally obtained as:

$$\begin{aligned} \tilde{u}_{i+\frac{1}{2},k} &= \frac{1}{R_{i+\frac{1}{2},k}} \left\{ (\widehat{Ru})_{i+\frac{1}{2},k}^n - \Delta t \left[(Ru \widehat{\nabla} \cdot \mathbf{Q})_{i+\frac{1}{2},k}^n \right] - (\widehat{\sqrt{g}})_{i+\frac{1}{2},k} \Delta t \left(\frac{\partial P}{\partial x} \right)_{i+\frac{1}{2},k}^n \right\} \\ \tilde{w}_{i,k+\frac{1}{2}} &= \frac{1}{R_{i,k+\frac{1}{2}}} \left\{ (\widehat{Rw})_{i,k+\frac{1}{2}}^n - \Delta t \left[(Rw \widehat{\nabla} \cdot \mathbf{Q})_{i,k+\frac{1}{2}}^n \right] - \Delta t \left(\frac{\partial P}{\partial \zeta} \right)_{i,k+\frac{1}{2}}^n \right\} \end{aligned} \quad (11)$$

In the second step momentum equations are again solved, with the pressure term approximated implicitly to remove stability restrictions due to the sound speed (Casulli, 1990; Casulli and Greenspan, 1984; Patnaik *et al.*, 1987); the momentum equation (x -direction) becomes

$$\frac{(Ru)_{i+\frac{1}{2},k}^{n+1} - (\widehat{Ru})_{i+\frac{1}{2},k}^n}{\Delta t} + (Ru \widehat{\nabla} \cdot \mathbf{Q})_{i+\frac{1}{2},k}^n = -(\sqrt{g})_{i+\frac{1}{2},k}^{n+1} \frac{(P_{i+1,k}^{n+1} - P_{i,k}^{n+1})}{\Delta x_{i+1/2}} \quad (12)$$

with $\Delta x_{i+1/2} = x_{i+1} - x_i$. By simple algebraic operations and substituting equation (11) into equation (12), we get the corrected values of $u_{i+\frac{1}{2},k}^{n+1}$:

$$u_{i+\frac{1}{2},k}^{n+1} = \tilde{u}_{i+\frac{1}{2},k} - \frac{\sqrt{g}^{n+1} \Delta t}{R_{i+\frac{1}{2},k}^{n+1}} \left[\frac{(P_{i+1,k}^{n+1} - P_{i,k}^{n+1})}{\Delta x_{i+1/2}} - \left(\frac{\partial P}{\partial x} \right)_{i+\frac{1}{2},k}^n \right], \quad (13)$$

Stable method
for air motion
inside cylinders

where the following assumptions have been made: $\bar{R} = R^{n+1}$ and $(\sqrt{g}) = (\sqrt{g})^{n+1}$.
In the same way, the corrected values of $w_{i,k+\frac{1}{2}}^{n+1}$ are obtained as

$$w_{i,k+\frac{1}{2}}^{n+1} = \tilde{w}_{i,k+\frac{1}{2}} - \frac{\Delta t}{R_{i,k+\frac{1}{2}}^{n+1}} \left[\frac{(P_{i,k+1}^{n+1} - P_{i,k}^{n+1})}{\Delta \zeta_{k+1/2}} - \left(\frac{\partial P}{\partial \zeta} \right)_{i,k+\frac{1}{2}}^n \right], \quad (14)$$

with $\Delta \zeta_{k+1/2} = \zeta_{k+1} - \zeta_k$ and hence

$$W_{i,k+\frac{1}{2}}^{n+1} = \frac{1}{(\sqrt{g})^{n+1}} \left(w_{i,k+\frac{1}{2}}^{n+1} - (w_{grid})_{i,k+\frac{1}{2}}^{n+1} \right). \quad (15)$$

Accuracy of velocity is first order in time and second order in space under the same hypotheses made for density.

In the 3D case predictor values of velocity at the co-ordinate y , v , are obtained analogously to u .

3.3 Energy conservation equation

Let us write energy equation in the integral form

$$\iint_V \frac{1}{\sqrt{g}} \left[\frac{\partial(\sqrt{g}E)}{\partial t} \right] dV + \iint_V \frac{1}{\sqrt{g}} \{ \nabla \cdot [\sqrt{g}(E+P)\mathbf{Q}] \} dV = - \iint_V \frac{1}{\sqrt{g}} \frac{\partial(Pw_{grid})}{\partial \zeta} dV; \quad (16)$$

since \sqrt{g} is constant over the volume cell, equation (16) results in

$$\begin{aligned} \iint_V \frac{1}{\sqrt{g}} \left[\frac{\partial(\sqrt{g}E)}{\partial t} \right] dV + \int_{l^+} (\sqrt{g}(E+P)u) d\zeta - \int_{l^-} (\sqrt{g}(E+P)u) d\zeta \\ + \int_{l^+} (\sqrt{g}(E+P)W) dx - \int_{l^+} (\sqrt{g}(E+P)W) dx \\ = - \int_{l^+} (Pw_{grid}) dx + \int_{l^+} (Pw_{grid}) dx. \end{aligned} \quad (17)$$

The following approximations will be made:

- (1) E constant in the cell in the volume integrals;
- (2) E , P , u and W constant over the boundaries of the cell in the line integrals;
- (3) upwind discretization of the time derivative;

- (4) explicit treatment of E and P in integrals;
- (5) implicit treatment of u and W in integrals.

Then equation (17) is approximated as

$$\begin{aligned}
 \frac{(\sqrt{g}E)_{i,k}^{n+1} - (\sqrt{g}E)_{i,k}^n}{\Delta t} V_{i,k} = & -[\sqrt{g}(E + P)]_{i+\frac{1}{2},k}^n u_{i+\frac{1}{2},k}^{n+1} \Delta \zeta_k \\
 & +[\sqrt{g}(E + P)]_{i-\frac{1}{2},k}^n u_{i-\frac{1}{2},k}^{n+1} \Delta \zeta_k \\
 & -[\sqrt{g}(E + P)]_{i,k+\frac{1}{2}}^n W_{i,k+\frac{1}{2}}^{n+1} \Delta x_i \\
 & +[\sqrt{g}(E + P)]_{i,k-\frac{1}{2}}^n W_{i,k-\frac{1}{2}}^{n+1} \Delta x_i \\
 & -P_{i,k+\frac{1}{2}}^n (w_{grid})_{i,k+\frac{1}{2}}^{n+1} \Delta x_i \\
 & +P_{i,k-\frac{1}{2}}^n (w_{grid})_{i,k-\frac{1}{2}}^{n+1} \Delta x_i. \tag{18}
 \end{aligned}$$

By using state equation $P = (\gamma - 1) \varrho \varepsilon$, we approximate total energy density by treating the kinetic energy term explicitly

$$E_{i,k}^{n+1} = \frac{P_{i,k}^{n+1}}{(\gamma - 1)} + \frac{1}{2} \varrho_{i,k}^{n+1} (|\tilde{\mathbf{q}}|_{i,k}^n)^2. \tag{19}$$

In order to improve accuracy, we let

$$\begin{aligned}
 \frac{(\sqrt{g}\tilde{E})_{i,k} - (\sqrt{g}E)_{i,k}^n}{\Delta t} V_{i,k} = & -[\sqrt{g}(E + P)]_{i+\frac{1}{2},k}^n \tilde{u}_{i+\frac{1}{2},k} \Delta \zeta_k \\
 & +[\sqrt{g}(E + P)]_{i-\frac{1}{2},k}^n \tilde{u}_{i-\frac{1}{2},k} \Delta \zeta_k \\
 & -[\sqrt{g}(E + P)]_{i,k+\frac{1}{2}}^n \tilde{W}_{i,k+\frac{1}{2}} \Delta x_i \\
 & +[\sqrt{g}(E + P)]_{i,k-\frac{1}{2}}^n \tilde{W}_{i,k-\frac{1}{2}} \Delta x_i \\
 & -P_{i,k+\frac{1}{2}}^n (w_{grid})_{i,k+\frac{1}{2}}^{n+1} \Delta x_i \\
 & +P_{i,k-\frac{1}{2}}^n (w_{grid})_{i,k-\frac{1}{2}}^{n+1} \Delta x_i, \tag{20}
 \end{aligned}$$

and advance total energy density by solving equation (20) using FCT method (Boris and Oran, 1987). Then by substituting equations (13-15) and (19) into equation (18) and by equation (20) we obtain the system of linear equations (five-band structured in the 2D case)

$$\begin{aligned}
 & a_{i-1,k} P_{i-1,k}^{n+1} + a_{i,k-1} P_{i,k-1}^{n+1} + a_{i,k} P_{i,k}^{n+1} + a_{i+1,k} P_{i+1,k}^{n+1} + a_{i,k+1} P_{i,k+1}^{n+1} \\
 &= (\sqrt{g}E)_{i,k} V_{i,k} - (\sqrt{g}E_c)_{i,k} V_{i,k} + a_{i+1,k} \left(\frac{\partial P}{\partial x} \right)_{i+\frac{1}{2},k}^n \Delta x_{i+1/2} \\
 &\quad - a_{i-1,k} \left(\frac{\partial P}{\partial x} \right)_{i-\frac{1}{2},k}^n \Delta x_{i-1/2} + a_{i,k+1} \left(\frac{\partial P}{\partial \zeta} \right)_{i,k+\frac{1}{2}}^n \Delta \zeta_{k+1/2} \\
 &\quad - a_{i,k-1} \left(\frac{\partial P}{\partial \zeta} \right)_{i,k-\frac{1}{2}}^n \Delta \zeta_{k-1/2}
 \end{aligned} \tag{21}$$

where the coefficients $a_{i,k}$ are defined as

$$\begin{aligned}
 a_{i-1,k} &= -\frac{\Delta t^2 [\sqrt{g}(E+P)]_{i-\frac{1}{2},k}^n \Delta \zeta_k}{R_{i-\frac{1}{2},k}^{n+1} \Delta x_{i-1/2}} \\
 a_{i,k-1} &= -\frac{\Delta t^2 [\sqrt{g}(E+P)]_{i,k-\frac{1}{2}}^n \Delta x_i}{(\sqrt{g})_{i,k-\frac{1}{2}}^{n+1} R_{i,k-\frac{1}{2}}^{n+1} \Delta \zeta_{k-1/2}} \\
 a_{i+1,k} &= -\frac{\Delta t^2 [\sqrt{g}(E+P)]_{i+\frac{1}{2},k}^n \Delta \zeta_k}{R_{i+\frac{1}{2},k}^{n+1} \Delta x_{i+1/2}} \\
 a_{i,k+1} &= -\frac{\Delta t^2 [\sqrt{g}(E+P)]_{i,k+\frac{1}{2}}^n \Delta x_i}{(\sqrt{g})_{i,k+\frac{1}{2}}^{n+1} R_{i,k+\frac{1}{2}}^{n+1} \Delta \zeta_{k+1/2}} \\
 a_{i,k} &= \frac{1}{(\gamma-1)} - a_{i-1,k} - a_{i,k-1} - a_{i+1,k} - a_{i,k+1}.
 \end{aligned} \tag{22}$$

They represent the five non-null coefficients of the matrix obtained allowing i, k to range over their own values in order to cover the whole domain.

The numerical solution of the system (21) allows one to obtain values of pressure, P , at time t^{n+1} . As far as accuracy of the numerical solution of energy equation is concerned, the same arguments as density and velocity apply. Finally, the scheme used is conservative.

In the 3D case convective terms across the co-ordinate y are included analogously.

3.4 Momentum equations (correction step)

In this step we can finally obtain the corrected values of the velocities, u and w , at time t^{n+1} by substituting the values of the pressure, P , at the new time into equations (13) and (14). After these corrections we can calculate the values of the total density energy, E , at time t^{n+1} by using the state equation (19), with velocity considered at time t^{n+1} .

3.5 General scheme of the procedure

Summarizing, the procedure for advancing variables from time t^n to time t^{n+1} goes through the following steps:

- (1) advance density (through mass conservation equation), by solving the system of linear equation (8); values of density at time t^{n+1} are obtained at the end of this step;
- (2) calculate predictor values of velocity by a semi-Lagrangian technique applied to the momentum equation (11);
- (3) advance pressure (through energy equation), by solving the system of linear equation (21); values of pressure are obtained at the end of this step;
- (4) correct values of velocity by means of equations (13) and (14) and of the total energy density by means of equation (19), considering velocity at time t^{n+1} . Velocity and total energy density at time t^{n+1} are obtained at the end of this step.

4. Computational topics

In this section we show some computational topics concerning the implementation of the method when applied to the engine problem.

4.1 The semi-lagrangian step

The present subsection concerns with the calculation of the term \hat{s} at the beginning of the characteristic curve (time t^n) ending at a point (x, ζ) at time t^{n+1} . According to Casulli (1987), we approximate the material derivative as

$$\frac{ds}{dt} \approx \frac{s(x_i, \zeta_k; t^{n+1}) - s(\hat{x}_i, \hat{\zeta}_k; t^n)}{\Delta t}$$

with $(\hat{x}_i, \hat{\zeta}_k)$ being the origin of the characteristic curve at t^n ending at (x_i, ζ_k) at t^{n+1} . This point is approximately obtained solving the following system of differential equations at time t^n

$$\begin{cases} \frac{dx}{dt} = u(x, \zeta, t) \\ \frac{d\zeta}{dt} = W(x, \zeta, t) \end{cases} \quad (23)$$

with initial conditions $x(t^{n+1}) = x_i, \zeta(t^{n+1}) = \zeta_k$

Velocity field is not constant both in space and in time. However, we will make the approximation that velocity in the system (23) is constant with respect to time and equal to the value at $t = t^n$. A simple Euler's method will be used to solve the system (23)

$$\begin{cases} x^{(m)} = x^{(m-1)} - u(x^{(m-1)}, \zeta^{(m-1)}) \tau \\ \zeta^{(m)} = \zeta^{(m-1)} - W(x^{(m-1)}, \zeta^{(m-1)}) \tau \end{cases} \quad \text{for } m = 1, 2, \dots, N-1, N \quad (24)$$

with $\tau = \Delta t/N$.

Accuracy in time of the simple Euler's method is of the same order (in t) as the whole numerical method. N has been chosen so that local Courant number is less than 1

$$\left| \frac{u\tau}{\Delta x} \right| \leq 1, \quad \left| \frac{W\tau}{\Delta \zeta} \right| \leq 1.$$

In the 3D case the system (23) includes a third equation for the co-ordinate y .

4.2 Interpolation

Both for calculating values of the variables at the beginning of the characteristic curve (e.g. \mathfrak{B}) and values of (u, w) in equations (13) and (14), it is needed to interpolate fields of variables in points different from the grid-points. To this purpose, a simple bilinear interpolation has been implemented (see Figure 4), which preserves monotonicity of the variables

$$s(x, \zeta) = (1 - p) [(1 - q) s_{i,k} + q s_{i,k-1}] + p [(1 - q) s_{i-1,k} + q s_{i-1,k-1}]$$

with

$$x_{i-1} \leq x \leq x_i, \quad \zeta_{k-1} \leq \zeta \leq \zeta_k, \quad p = x - x_{i-1} \text{ and } q = \zeta - \zeta_{k-1}.$$

In the 3D case a trilinear interpolation formula is defined analogously.

4.3 Solution of the pressure system equation

The most time-consuming operation to be performed in the implementation of the code is the solution of the system of linear equations (21) in the unknown pressure. This task is very important, since overall computational efficiency and stability mainly depend on it. For this reason it is very important that the resulting matrix has nice properties from the theoretical and computational point of view. This is indeed the case of matrix (22). In fact, it is band-structured (3 bands in 1D, 5 bands in 2D, 7 bands in 3D and in all cases block tridiagonal); moreover, it is symmetric, strictly diagonal dominant with the special feature

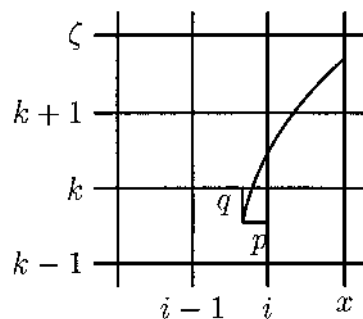


Figure 4.
Bilinear interpolation

that $a_{i,i} > 0$ and $a_{i,j} \leq 0$, with $i \neq j$ (in mathematical formalism it is a Z -matrix). The important consequence from the theoretical point of view is that a unique solution exists and stability of the numerical solution method can be easily guaranteed. Moreover, from the computational point of view the properties of the matrix make powerful solvers, like conjugate gradients, very effective. In the present paper a simple diagonal preconditioner was considered; any progress in this field can only improve efficiency of the method. Tests on several present and new preconditioners are in progress. We notice that the so nice properties of the matrix are very strongly dependent on the numerical approximations. As an example, it could be shown that approximation of the energy equation in its differential, rather than integral, form does not produce a symmetric, strictly diagonal dominant matrix.

4.4 Other topics

Implementation of the numerical method does not give particular problems. The language chosen for the code is Fortran. Memory occupation is about 7MB for a maximum of 20,000 grid points, with no particular optimization of the code. As a reference, memory occupation of the KIVA code for the same number of grid points is about 18MB. We want also to notice that the code can be easily vectorized in most parts and some of them are well suited for parallelization (e.g. the semi-lagrangian step).

5. Stability of the method

It is well known that stability is a very important property of a numerical method. Unfortunately current tools for analyzing stability can be applied only to very simple problems, with the consequence that strong (often unrealistic) hypotheses are made on the physical system in order to develop stability analysis on complicated equations. The same arguments apply also to the present numerical method.

Let us first consider the matrix involved in the numerical method for the mass conservation equation (see section 3.1); classical Von Neumann analysis shows that computation of density is unconditionally stable.

Let us now consider the matrix obtained approximating momentum and energy equations (see section 3.3); arguments of section 4.3 pressure provide a *de facto* stability of the method without making assumptions of periodicity and linearity which are currently made in theoretical analysis. This result was achieved by forcing the method to produce suitable matrices in the system of linear equations. However, for the sake of completeness, we shall also work out a theoretical stability analysis according to the Von Neumann method; to this purpose we shall follow guidelines of Casulli (1990). We assume that Euler equations are linear and defined with periodic boundary conditions on a finite domain; moreover we suppose a uniform grid, with spacing Δx and $\Delta \zeta$ constant. Hence, the difference equations (8), (13-14) and (18) reduce to

$$\begin{aligned}
 & (1 + 2\nu_i + 2\nu_k)R_{i,k}^{n+1} + \frac{1}{2}\epsilon_i(R_{i+1,k}^{n+1} - R_{i-1,k}^{n+1}) - \nu_i(R_{i+1,k}^{n+1} + R_{i-1,k}^{n+1}) \\
 & + \frac{1}{2}\epsilon_k(R_{i,k+1}^{n+1} - R_{i,k-1}^{n+1}) - \nu_k(R_{i,k+1}^{n+1} + R_{i,k-1}^{n+1}) = R_{i,k}^n \\
 (Ru)_{i+\frac{1}{2},k}^{n+1} + \sqrt{g} \frac{\Delta t}{\Delta x} (P_{i+1,k}^{n+1} - P_{i,k}^{n+1}) &= (\widehat{Ru})_{i+\frac{1}{2},k}^n \left[1 - \Delta t(\widehat{\nabla} \cdot \mathbf{Q})_{i+\frac{1}{2},k}^n \right] \\
 (Rw)_{i,k+\frac{1}{2}}^{n+1} + \frac{\Delta t}{\Delta \zeta} (P_{i,k+1}^{n+1} - P_{i,k}^{n+1}) &= (\widehat{Rw})_{i,k+\frac{1}{2}}^n \left[1 - \Delta t(\widehat{\nabla} \cdot \mathbf{Q})_{i,k+\frac{1}{2}}^n \right] \\
 (P')_{i,k}^{n+1} + (\gamma - 1) \frac{(E' + P')}{R} \frac{\Delta t}{\Delta x} &\left[(Ru)_{i+\frac{1}{2},k}^{n+1} - (Ru)_{i-\frac{1}{2},k}^{n+1} \right] \\
 + \frac{(\gamma - 1)(E' + P')}{\sqrt{g} R} \frac{\Delta t}{\Delta \zeta} &\cdot \left[(Rw)_{i,k+\frac{1}{2}}^{n+1} - (Rw)_{i,k-\frac{1}{2}}^{n+1} \right] \\
 = (P')_{i,k}^n - \left[\frac{P'(\gamma-1)}{\sqrt{g}} - \frac{(\gamma-1)(E' + P')}{\sqrt{g}} \right] &\frac{\Delta t}{\Delta \zeta} \Delta(w_{grid})^{n+1} \quad (25)
 \end{aligned}$$

where $(S)_{i,k}^n = \sqrt{g} S$ (S being a generic variable) and all the coefficients have been assumed constant. Now, by changing variable P' with

$$\bar{P}(\sqrt{(E' + P')(\gamma - 1)}) / (\sqrt{g}, \sqrt{R})$$

and approximating the values calculated at the beginning of the characteristic, $\widehat{S}_{i,k}$ with a bilinear interpolation over the four surrounding grid points (for more details see the subsection 4.2) equations (25) become

$$\begin{aligned}
 & (1 + 2\nu_i + 2\nu_k)R_{i,k}^{n+1} + \frac{1}{2}\epsilon_i(R_{i+1,k}^{n+1} - R_{i-1,k}^{n+1}) - \nu_i(R_{i+1,k}^{n+1} + R_{i-1,k}^{n+1}) \\
 & + \frac{1}{2}\epsilon_k(R_{i,k+1}^{n+1} - R_{i,k-1}^{n+1}) - \nu_k(R_{i,k+1}^{n+1} + R_{i,k-1}^{n+1}) = R_{i,k}^n \\
 (Ru)_{i+\frac{1}{2},k}^{n+1} + \frac{\Delta t}{\Delta x} \frac{\sqrt{(E' + P')(\gamma - 1)}}{\sqrt{R}} &(\bar{P}_{i+1,k}^{n+1} - \bar{P}_{i,k}^{n+1}) = (1 - p) \left[(1 - q)(Ru)_{i+\frac{1}{2}-n,k-m}^n \right. \\
 & \left. + q(Ru)_{i+\frac{1}{2}-n,k-m-1}^n \right] + p \left[(1 - q)(Ru)_{i-\frac{1}{2}-n,k-m}^n + q(Ru)_{i-\frac{1}{2}-n,k-m-1}^n \right] \\
 (Rw)_{i,k+\frac{1}{2}}^{n+1} + \frac{\Delta t}{\Delta \zeta} \frac{\sqrt{(E' + P')(\gamma - 1)}}{\sqrt{g} \sqrt{R}} &(\bar{P}_{i,k+1}^{n+1} - \bar{P}_{i,k}^{n+1}) = (1 - p) \left[(1 - q)(Rw)_{i-n,k+\frac{1}{2}-m}^n \right. \\
 & \left. + q(Rw)_{i-n,k-\frac{1}{2}-m}^n \right] + p \left[(1 - q)(Rw)_{i-n-1,k+\frac{1}{2}-m}^n + q(Rw)_{i-n-1,k-\frac{1}{2}-m}^n \right] \\
 (\bar{P})_{i,k}^{n+1} + \frac{\sqrt{(E' + P')(\gamma - 1)}}{\sqrt{R}} \frac{\Delta t}{\Delta x} &\left[(Ru)_{i+\frac{1}{2},k}^{n+1} - (Ru)_{i-\frac{1}{2},k}^{n+1} \right] \\
 + \frac{\sqrt{(E' + P')(\gamma - 1)}}{\sqrt{g} \sqrt{R}} \frac{\Delta t}{\Delta \zeta} &\left[(Rw)_{i,k+\frac{1}{2}}^{n+1} - (Rw)_{i,k-\frac{1}{2}}^{n+1} \right] = (\bar{P})_{i,k}^n,
 \end{aligned}$$

with $a = (x_{i+\frac{1}{2}} - \bar{x})/\Delta x$, $b = (\zeta_{k+\frac{1}{2}} - \bar{\zeta})/\Delta \zeta$. We want to notice that a and b could be not integers, i.e. $a = n + p$, $b = m + q$, where n and m are integers and $0 \leq p < 1$, $0 \leq q < 1$.

By considering usual Fourier modes,

$$\widehat{R}e^{j(i\alpha + k\beta)}, p e^{j(i\alpha + k\beta)}, (\widehat{Ru})e^{j(i+\frac{1}{2})\alpha + k\beta}, (\widehat{Rw})e^{j(i\alpha + (k+\frac{1}{2})\beta)},$$

with $j = \sqrt{-1}$, evaluated at the proper positions in the grid of the corresponding variables, we obtain

$$\begin{aligned} & \widehat{R}^{n+1} \left[1 + 2\nu_i + 2\nu_k + \frac{1}{2}\epsilon_i(e^{j\alpha} - e^{-j\alpha}) - \nu_i(e^{j\alpha} + e^{-j\alpha}) \right. \\ & \quad \left. + \frac{1}{2}\epsilon_k(e^{j\beta} - e^{-j\beta}) - \nu_k(e^{j\beta} + e^{-j\beta}) \right] = \widehat{R}^n \\ & (\widehat{Ru})^{n+1} + \frac{\Delta t}{\Delta x} \frac{\sqrt{(E' + P')(\gamma - 1)}}{\sqrt{R}} (e^{j\alpha/2} - e^{-j\alpha/2}) \widehat{P}^{n+1} \\ & = (\widehat{Ru})^n e^{-jn\alpha} e^{-jm\beta} [(1 - p) + pe^{-j\alpha}] [(1 - q) + qe^{-j\beta}] \\ & (\widehat{Rw})^{n+1} + \frac{\Delta t}{\Delta \zeta} \frac{\sqrt{(E' + P')(\gamma - 1)}}{\sqrt{g} \sqrt{R}} (e^{j\beta/2} - e^{-j\beta/2}) \widehat{P}^{n+1} \\ & = (\widehat{Rw})^n e^{-jn\alpha} e^{-jm\beta} [(1 - p) + pe^{-j\alpha}] [(1 - q) + qe^{-j\beta}] \\ & \widehat{P}^{n+1} + \frac{\sqrt{(E' + P')(\gamma - 1)}}{\sqrt{R}} \frac{\Delta t}{\Delta x} (e^{j\alpha/2} - e^{-j\alpha/2}) (\widehat{Ru})^{n+1} \\ & + \frac{\sqrt{(E' + P')(\gamma - 1)}}{\sqrt{g} \sqrt{R}} \frac{\Delta t}{\Delta \zeta} (e^{j\beta/2} - e^{-j\beta/2}) (\widehat{Rw})^{n+1} = \widehat{P}^n, \end{aligned}$$

that is

$$\begin{aligned} \widehat{R}^{n+1} &= C_1 \widehat{R}^n \\ (\widehat{Ru})^{n+1} + 2jH\widehat{P}^{n+1} &= C_2 (\widehat{Ru})^n \\ (\widehat{Rw})^{n+1} + 2jK\widehat{P}^{n+1} &= C_2 (\widehat{Rw})^n \\ \widehat{P}^{n+1} + 2jH(\widehat{Ru})^{n+1} + 2jK(\widehat{Rw})^{n+1} &= \widehat{P}^n, \end{aligned} \tag{26}$$

where we assume that

$$C_1 = [1 + 2\nu_i(1 - \cos \alpha) + 2\nu_k(1 - \cos \beta) + j(\epsilon_i \sin \alpha + \epsilon_k \sin \beta)]^{-1},$$

$$C_2 = [\cos n\alpha - j \sin n\alpha][\cos m\beta - j \sin m\beta][1 - p + p(\cos \alpha - j \sin \alpha)][1 - q + q(\cos \beta - j \sin \beta)]$$

$$H = \frac{\sqrt{(E' + P')(\gamma - 1)}}{\sqrt{R}} \frac{\Delta t}{\Delta x} \sin \frac{\alpha}{2}$$

$$K = \frac{\sqrt{(E' + P')(\gamma - 1)}}{\sqrt{g} \sqrt{R}} \frac{\Delta t}{\Delta \zeta} \sin \frac{\beta}{2}.$$

In matrix notation equation (26) can be written as

$$B\hat{\mathbf{x}}^{n+1} = D\hat{\mathbf{x}}^n \quad (27)$$

Stable method
for air motion
inside cylinders

where $\hat{\mathbf{x}}^n = [\hat{r}^n, \hat{R}U^n, \hat{R}W^n, \hat{P}^n]^T$ and

$$B = \begin{pmatrix} 1 & 0 & 0 & 0 \\ 0 & 1 & 0 & 2jH \\ 0 & 0 & 1 & 2jK \\ 0 & 2jH & 2jK & 1 \end{pmatrix}, \quad D = \begin{pmatrix} C_1 & 0 & 0 & 0 \\ 0 & C_2 & 0 & 0 \\ 0 & 0 & C_2 & 0 \\ 0 & 0 & 0 & 1 \end{pmatrix}.$$

881

Since B is not singular (e.g. $\|B\|_2 \neq 0$), equation (27) results in

$$\hat{\mathbf{x}}^{n+1} = G\hat{\mathbf{x}}^n \quad (28)$$

where $G = B^{-1}D$ is the amplification matrix of the method. A necessary and sufficient condition for stability is

$$\frac{\|\hat{\mathbf{x}}^{n+1}\|_2}{\|\hat{\mathbf{x}}^n\|_2} = \|G\|_2 \leq 1$$

identically for every α and β . But, since $\|G\|_2 \leq \|B^{-1}\|_2 \|D\|_2$, we can seek the sufficient conditions $\|B^{-1}\|_2 \leq 1$ and $\|D\|_2 \leq 1$. The two matrices B and D , and hence B^{-1} , are normal matrices. Thus their norms are equal to their corresponding spectral radii. By solving the characteristic equation of B (that is $\det(B - \lambda I) = (1 - \lambda)^2[(1 - \lambda)^2 + 4(H^2 + K^2)] = 0$), we obtain the eigenvalues of B : $\lambda_1 = \lambda_2 = 1$, $\lambda_3 = 1 + 2j\sqrt{H^2 + K^2}$ and $\lambda_4 = 1 - 2j\sqrt{H^2 + K^2}$. One can note that the spectral radius of B is always no less than unity, and hence that of B^{-1} is always no greater than unity. Next, the eigenvalues of D are: $\lambda_1 = C_1$, $\lambda_2 = \lambda_3 = C_2$ and $\lambda_4 = 1$; after some simplifications, we obtain $|C_2| = |1 + 2(\rho^2 - \rho)(1 - \cos\alpha)| |1 + 2(q^2 - q)(1 - \cos\beta)|$. Being $0 \leq \rho, q \leq 1$, we get $|C_2| \leq 1$ for every α and β ; hence, since $|C_1| \leq 1$, the spectral radius of D is always no greater than unity. Therefore the numerical method is unconditionally stable.

In the 3D case it is possible to show that stability analysis can be worked out by a straightforward extension of the 2D case and gives the same results of unconditional stability.

6. Numerical experiments

The numerical method described before has been implemented, and some numerical experiments were carried out in order to show its performance. A test-case is considered referring to a vertical section of a cylindrical bowl with its axis coincident with the axis of the cylinder; in the present paper we show only results obtained for engine parameters shown in Table I. All runs were performed at engine speed 1,250rpm, with a starting swirl ratio equal to 0, with

HFF
8,8

slip boundary conditions and piston starting at 90° BTDC (i.e. before the end of the compression stroke). The initial values of the system variables are constant inside the cylinder and depend on the starting position; moreover no initial motion is supposed there, while on the walls the velocities depend on the piston speed. Adiabatic walls were considered.

882

Aim of the tests is to understand the effects of the maximum Courant number (with respect to the fluid speed) and of the grid resolution on the results and on the execution time. Five different executions were made by choosing a maximum Courant number equal to 0.5, 1, 2, 5 and 10, respectively; moreover two different grid resolutions were considered. In the first case a resolution of 50 gridpoints for each coordinate was considered ($\Delta x = \Delta z = 0.002\text{m}$, for a total of 2,200 actual gridpoints), while in the second one we considered a resolution of 100 gridpoints for each coordinate ($\Delta x = \Delta z = 0.001\text{m}$, for a total of 8,800 actual gridpoints). All runs were made on an IBM Power2 Risc 58H. Execution times from 90° BTDC to TDC are shown in Table II for both resolutions. They are promising with respect to the typical times of well assessed codes for engines (as a reference, a run for the same geometry and resolution 50 grid points for each coordinate takes 1 hour 7 minutes). Also we note that an increase of resolution involves a corresponding increase of the execution time, while accuracy becomes better. Figures 5-8 show the velocity field in the first test-case at TDC obtained with a maximum Courant number of 0.5, 1, 2 and 5, respectively. Figures 9-12 show the same results in the second test-case.

The main conclusion that can be drawn is that the numerical method is stable also for high Courant numbers. Moreover, simulations of air flow field are similar at all the Courant numbers considered, especially when spatial resolution improves. Note from Table II that for increasing Courant numbers there is not a corresponding effective abatement of execution speed, so that it is advisable from a practical point of view not to choose Courant numbers greater than five, since gain of execution speed is negligible, while accuracy decreases. Saturation of the execution speed with the Courant number is due to two

Table I.
Physical parameters of the engine system simulated for the numerical experiments

Bowl diameter m	Bowl height m	Cylinder diameter m	Squish m	Stroke m	Connecting rod length m
0.06	0.03	0.1	0.005	0.065	0.11

Table II.
Execution times for different maximum Courant numbers in both test-cases

Maximum Courant number	0.5	1	2	5	10
50 gridpoints/coordinate	1hr 05mins	50mins	35mins	25min	15mins
100 gridpoints/coordinate	11hr 30mins	8hr 45mins	5hr 55mins	4hr 30mins	3hr 35mins

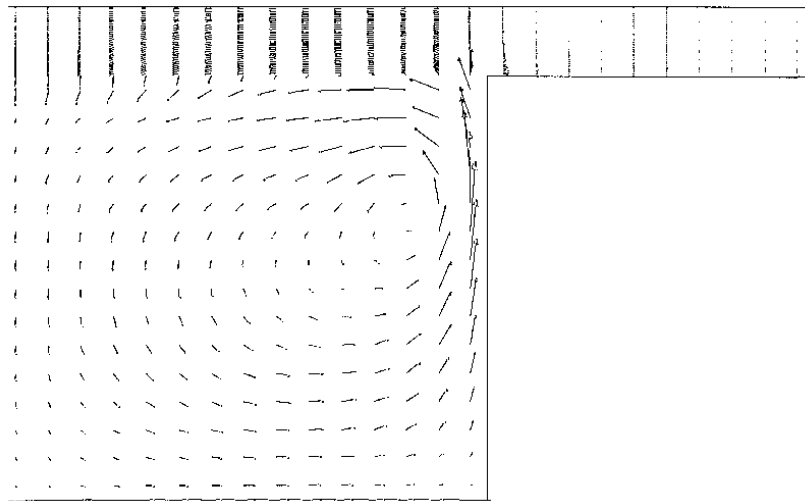


Figure 5.
Flow field for engine
parameters shown in
Table I at TDC and a
resolution of 50 grid
points/coordinate for a
maximum Courant
number 0.5

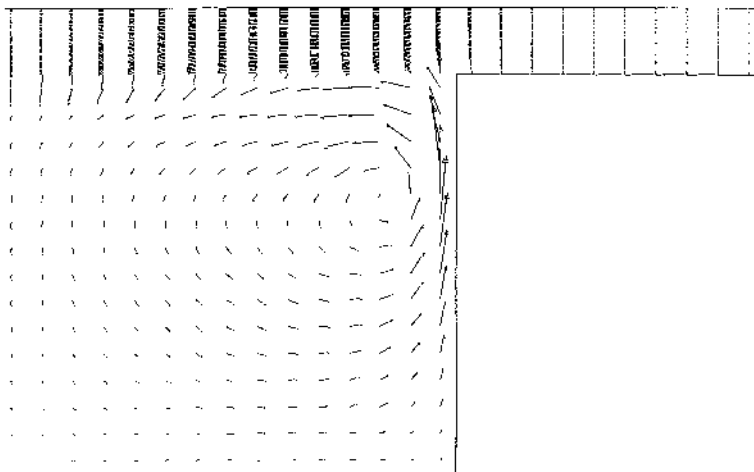


Figure 6.
Flow field for engine
parameters shown in
Table I at TDC and a
resolution of 50 grid
points/coordinate for a
maximum Courant
number 1

reasons: from on side the semi-lagrangian step does not involve significant reduction of the execution time (see subsections 3.2 and 4.1); moreover a higher number of iterations is required for solving the linear systems due to a worse starting solution of the iterative procedure (a suitable preconditioner of the CG method could be useful to this purpose).

Finally we compared the results obtained with our code with those given by the KIVA code on the same engine parameters shown in Table I; to this purpose the KIVA code was organized so to simulate equation (1) as much as possible, that is not considering viscosity, turbulence, combustions and so on. As an example in Figure 13 we show air flow field as obtained at TDC with a grid

HFF
8,8

884

Figure 7.
Flow field for engine parameters shown in Table I at TDC and a resolution of 50 grid points/coordinate for a maximum Courant number 2

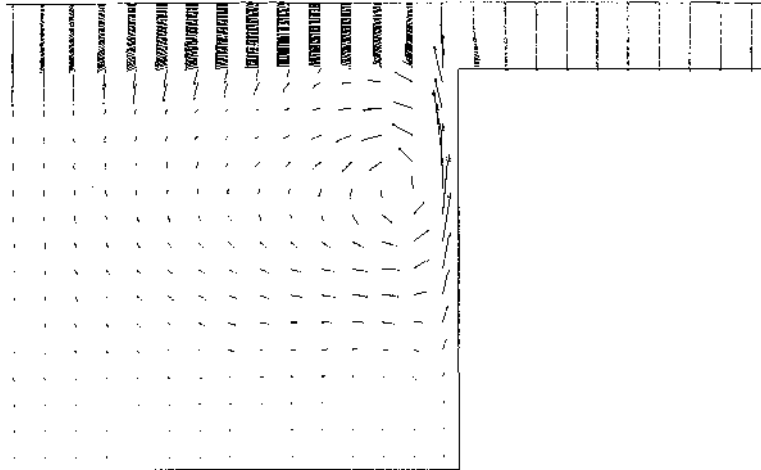
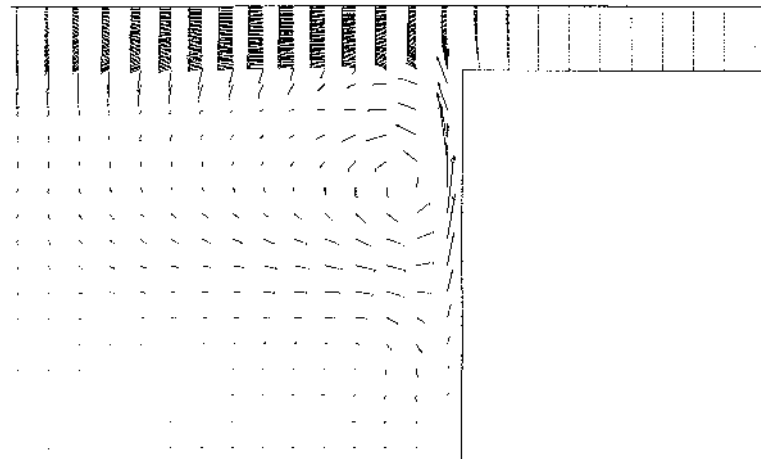


Figure 8.
Flow field for engine parameters shown in Table I at TDC and a resolution of 50 grid points/coordinate for a maximum Courant number 5



resolution of 50 gridpoints for each co-ordinate; comparison with the analogous plots of Figures 5-8 is quite favourable.

7. Conclusions

In the present paper we developed a mixed finite difference-finite volume implicit-semi lagrangian numerical method for simulating air motion inside cylinders of engines. The method considers 2D Cartesian domains, but extension to 3D and/or cylindrical coordinates is immediate. The method is unconditionally stable; this objective has been reached by an implicit treatment of the computational density in the mass conservation equation and a semi-lagrangian treatment of total derivatives in the momentum equations (which removes stability restriction due to the fluid speed) and an implicit treatment of

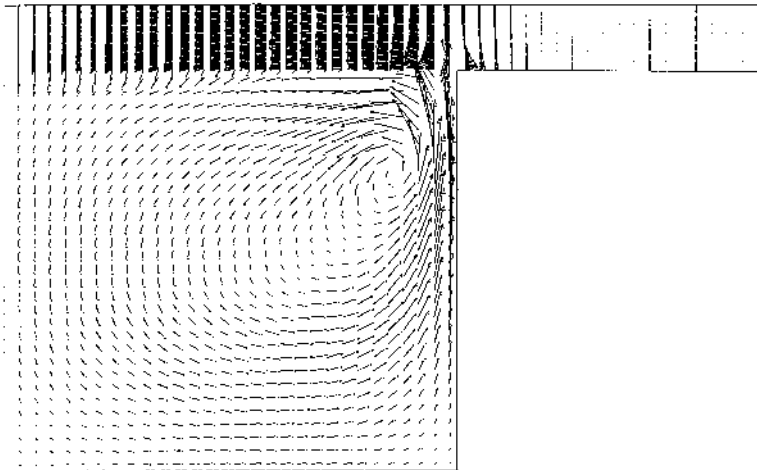


Figure 9.
Flow field for engine
parameters shown in
Table I at TDC and a
resolution of 100 grid
points/coordinate for a
maximum Courant
number 0.5

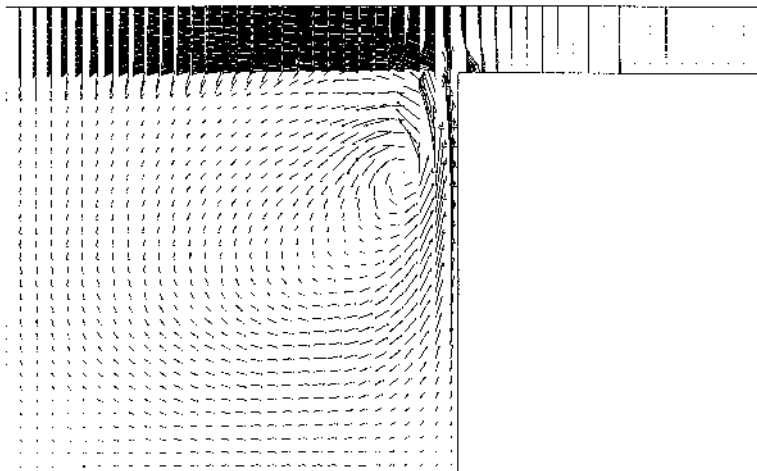


Figure 10.
Flow field for engine
parameters shown in
Table I at TDC and a
resolution of 100 grid
points/coordinate for a
maximum Courant
number 1

pressure terms in the momentum equations and velocity in the energy equation (which removes stability restriction due to the sound speed). Moreover, as many as possible physical properties of the engine system have been taken into account by the numerical method, namely conservation, positivity, monotonicity. Conservation of mass and energy was guaranteed by a finite-volume approximation of the corresponding equations; moreover positivity and monotonicity are obtained through a frequent use of nonlinear FCT method. Overall accuracy of the method is first order in time and second one in space where solution is smooth; due to FCT, space accuracy drops to the first order

HFF
8,8

886

Figure 11.
Flow field for engine
parameters shown in
Table I at TDC and a
resolution of 100 grid
points/coordinate for a
maximum Courant
number 2

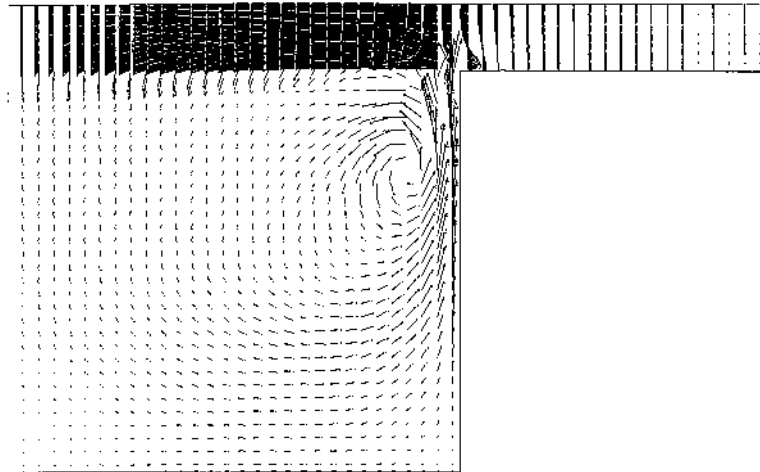
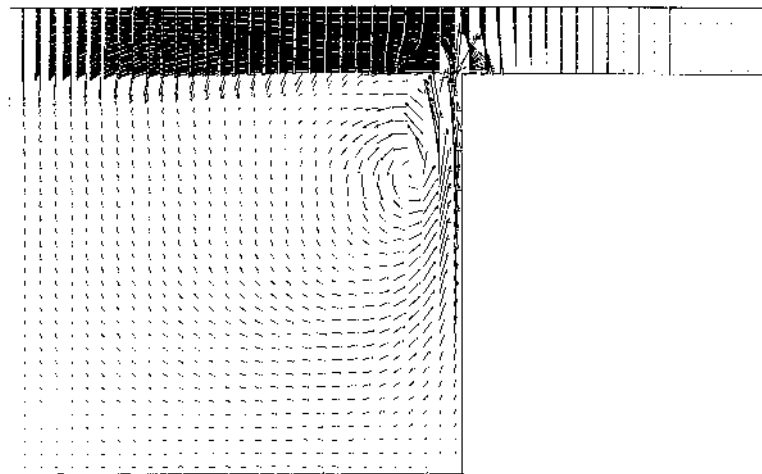


Figure 12.
Flow field for engine
parameters shown in
Table I at TDC and a
resolution of 100 grid
points/coordinate for a
maximum Courant
number 5



where solution is steep. Stability of the method has been proved both by a classical Von Neumann analysis and analysis of the matrix involved in the system of linear equations. In particular the nice mathematical structure of the matrices involved in the numerical methods makes the solution of corresponding systems very efficient. Finally, numerical experiments have been worked out in order to analyze the influence of the maximum Courant number (with respect to the fluid speed) on the overall performance of the numerical method.

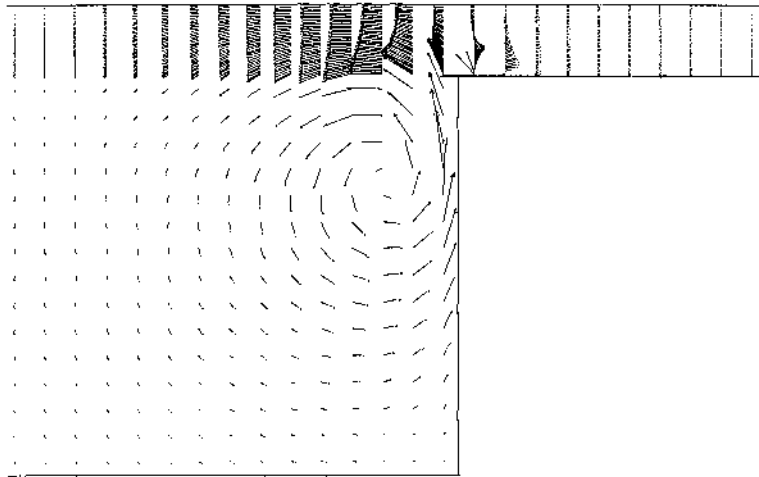


Figure 13.
Flow field for engine
parameters shown in
Table I at TDC and a
resolution of 50 grid
points/coordinate as
obtained by KIVA code

References

- Amsden, A.A., O'Rourke, P.J. and Butler, T.D. (1989), *KIVA II: A Computer Program for Chemically Reactive Flows with Sprays*, Los Alamos National Laboratory Report No. LA 11560-M5, Los Alamos, NM.
- Boris, J.P. and Oran, E.S. (1987), *Numerical Simulation of Reactive Flows*, Elsevier Science Publishing, Barking.
- Casulli, V. (1987), "Eulerian-Lagrangian methods for hyperbolic and convection dominated parabolic problems", in *Computational Methods for Non Linear Problems*, Pineridge Press, Swansea.
- Casulli, V. (1990), "Semi-implicit finite difference methods for the two-dimensional shallow water equations", *J. Comp. Phys.*, Vol. 86, pp. 56-74.
- Casulli, V. and Greenspan, D. (1984), "Pressure method for the numerical solution of transient, compressible fluid flows", *Int. J. Numerical Methods in Fluids*, Vol. 4, pp. 1001-12.
- Issa, R.I. (1986), "Solution of the implicitly discretised fluid flow equations by operator-splitting", *J. Comp. Phys.*, Vol. 62, pp. 40-65.
- Johns, R.J.R. (1984), *A Unified Method for Calculating Engine Flows*, ASME paper No. 84-DGP-18.
- Patnaik, G., Guirguis, R.H., Boris, J.P. and Oran, E.S. (1987), "A barely implicit correction for flux corrected transport", *J. Comp. Phys.*, Vol. 71, pp. 1-20.
- Thompson, J.F., Warsi, Z.U.A. and Mastin, C.W. (1985), *Numerical Grid Generation*, Elsevier Science Publishing, Barking.